Contribution from the Departament de Química Inorgànica, Universitat de Barcelona, Barcelona, Spain, Department of Chemistry, North Carolina State University, Raleigh, North Carolina, and Laboratoire de Chimie des Solides, Université de Nantes, Nantes, France

Electronic Structure, Bonding, and Properties of CuP_2

Pere Alemany,[†] Santiago Alvarez,*[,†] Myung-Hwan Whangbo,*[,‡] and Michel Evain[§]

Received March 21, 1991

A theoretical study of the electronic structure of CuP_2 is presented on the basis of molecular orbital and tight-binding band calculations based upon the extended Hückel method. We examined the electronic factors leading to ethane- and diborane-like coordination arrangements of dinuclear compounds and found the diborane-like coordination geometry of the d^{10} ions in CuP_2 to be favorable on electronic grounds. The analysis of DOS and COOP curves shows that there are two important contributions to Cu–Cu bonding: delocalized bonding involving the bridging phosphorus atoms in the Cu_2P_2 rings and through-space Cu(I)–Cu(I) interactions due to mixing of the occupied d_{z^2} and empty s and p_z orbitals. The electronic band structure of CuP_2 has a substantial energy gap between the valence and conduction bands. The valence band is dispersive along the interlayer direction due to the coupling of the metal d orbitals through the polyphosphide sublattice.

The MP_4 stoichiometry is probably the most common one for phosphorus-rich transition-metal polyphosphides and includes more than 17 compounds which crystallize in 11 different structural types.[1-4] In these MP_4 compounds, the phosphorus sublattice is formed by condensation of puckered ten-membered rings, which can be formally described as P_4^{2-}, and the transition-metal ion is octahedrally coordinated by the phosphorus atoms. The known structural types differ from one another by (a) the way in which the P_{10} rings are condensed, (b) the way in which the coordination octahedra are linked together, and (c) the existence or absence of metal–metal contacts to form either pairs or chains of metal atoms.

One of the structural types of tetraphosphides is the CdP_4 structure,[5-10] which is found for MgP_4, $MgAs_4$, and the α form of RuP_4 and OsP_4. The copper and silver diphosphides, CuP_2 and AgP_2, have a related structure.[11,12] These diphosphides present a phosphorus sublattice of the CdP_4 type, in which the octahedral site is occupied by a pair of metal atoms [Cu–Cu and Ag–Ag distances are 2.476 (1) and 2.816 (1) Å, respectively]. The MP_2 phosphides (M = Cu, Ag)[13,14] and their mononuclear analogues MP_4 (M = Cd, Ru, Os) have been found to be diamagnetic and semiconducting.[10,15]

Bonds between d^{10} ions are found in a number of solid-state compounds,[16] and unlike their molecular analogues, no theoretical analysis of such bonding in three-dimensional structures has been reported so far. A striking structural feature of CuP_2 and AgP_2 is the diborane-like geometry of the M–M pairs, not a familiar arrangement in extended structures. All these prompted us to study the electronic band structure of CuP_2. In what follows we first describe the general structure of the phosphorus sublattice and how the M_2 groups are connected to the phosphorus atoms. Then the electronic structures of CuP_2 and related compounds are studied with the help of molecular orbital and band structure calculations of the extended Hückel type, and their bonding and electrical properties are discussed.

Description of the Structures

Our starting point for a description of the structure of the P_4^{2-} sublattice is a P_4 layer **1** formed by fusing P_6 rings with boat conformation. Such layers differ slightly from those of black phosphorus,[17,18] in which the P_6 rings have a chair conformation. Shown in **2** is a P_4^{2-} layer that results from the P_4 layer **1** by adding two electrons thereby breaking one P–P bond per formula unit. This is the P_4^{2-} layer found in MP_4 (M = V, Cr, Mo).[19-21] Notice that the disconnected P–P bonds are related by the transition vectors *a* and 2*c*. Isomeric P_4^{2-} layers can be generated with a different choice of translation vectors, schematically shown in **3**,

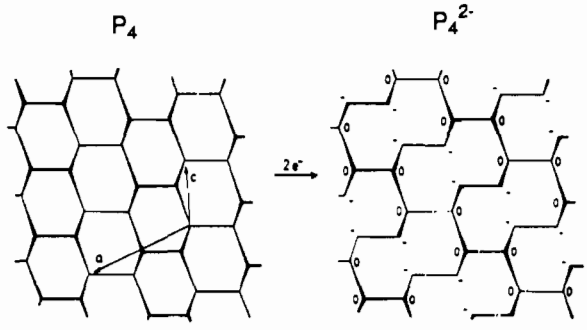

1 **2**

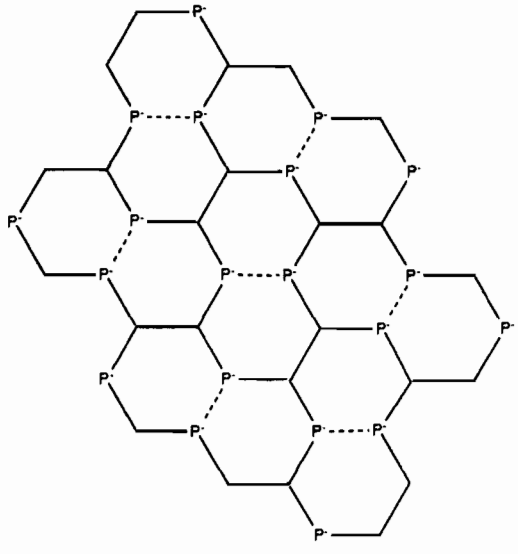

3

as found for CdP_4. The P_4^{2-} layer **3** consists of fused P_{10} rings with a double boat conformation, **4**, and has two kinds of phos-

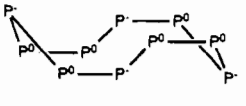

4

[†] Universitat de Barcelona.
[‡] North Carolina State University.
[§] Université de Nantes.

(1) Jeitschko, W.; Flörke, U.; Möller, M. H.; Rühl, R. *Ann. Chim. Fr.* **1982**, *7*, 525.

0020-1669/92/1331-0119$03.00/0

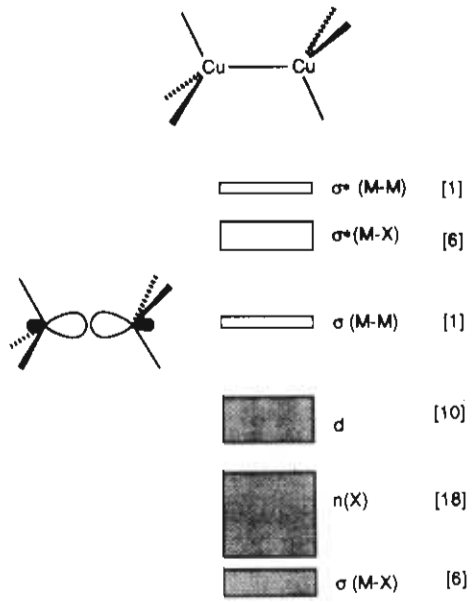

Figure 1. Block diagram of the molecular orbitals of $[Cu_2Br_6]^{4-}$ with an ethane-like staggered structure. Shaded blocks corresponded to filled orbitals. The numbers in square brackets indicate the number of orbitals within each block.

phorus atoms in each P_{10} ring: six P^0 atoms shared by three rings bear one lone pair, whereas four P^- atoms shared by two rings bear two lone pairs.

The metal ions in the CdP_4 structure are sandwiched between the P_4^{2-} layers **3**. It is clear from **4** that one metal atom can sit at the center of each of the boats, coordinated by one P^0 and two P^- atoms of a P_{10} ring in a *fac* arrangement. In order to complete the octahedral coordination of the metal ion, the next phosphorus layer **3** must be shifted as shown in **5**, resulting in a monoclinic system.

If we substitute the Cd^{2+} ions in the CdP_4 structure with M_2 pairs [M = Cu(I), Ag(I)], an $(M_2)P_4$ formula unit results. In principle, the coordination environment of an M_2 pair can be either ethane-like, **6a**, or diborane-like, **6b**. CuP_2 and AgP_2 are found

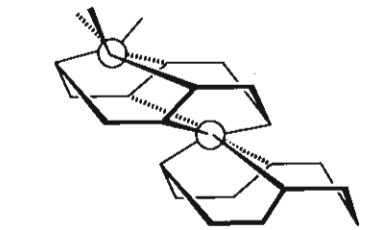

5

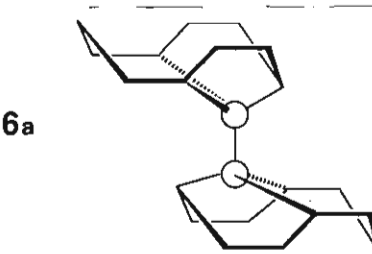

6a

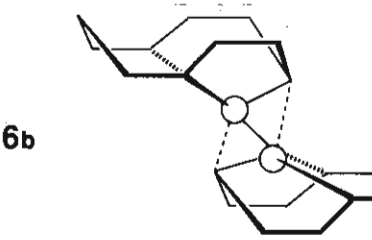

6b

to adopt the arrangement **6b**. As shown in **7**, each metal atom

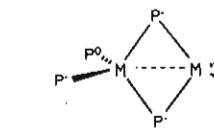

7

is surrounded by four phosphorus atoms in an approximately tetrahedral fashion, with the two tetrahedra sharing an edge. The bridging atoms are of P^- type. The M–M distances are 2.476 and 2.816 Å for M = Cu and Ag, respectively, comparable to the corresponding Cu(I)–Cu(I) bonding distances in solid-state[16] or in molecular complexes.[22,23] There are several Cu(I) compounds with diborane structures in which the copper atoms are bridged by X or XR groups.[24] Only in $[Cu(PMe_3)_2(\mu\text{-}SbR_2)]_2$ and in the CuP_2 structure the bridging groups are of the XR_2 or XR_3 type.[25] In the latter case, the bridging P^- atoms are linked to two other P atoms (see **6b**) and coordinated to a Cu atom as a terminal ligand and can be therefore considered as a PR_3 group.

Cu–Cu Bonding in a Model Cu_2X_6 Molecule

The weak metal–metal bonding present in nonbridged dinuclear complexes of d^{10} ions has been theoretically analyzed previously.[23,26-30] Such bonds are due to second-order mixing of the occupied d_{z^2} and the empty s and p_z orbitals, which results in a hybridization of the σ combination of d_{z^2} toward, and of their σ^* combination away from, the interior of the metal–metal region, as depicted in **8**. However, the metal atoms in CuP_2 and AgP_2 are bridged by phosphorus atoms, and it has been recently shown[24] that in dinuclear Cu(I) compounds with bridging ligands the Cu–Cu interaction is a delocalized one as in diborane, with only

(2) Hulliger, R. *Struct. Bonding* **1968**, 83.
(3) Schnering, H.-G. v.; Hönle, W. *Chem. Rev.* **1988**, *88*, 243.
(4) Evain, M.; Brec, R.; Fiechter, S.; Tributsch, H. *J. Solid State Chem.* **1987**, *71*, 40.
(5) Krebs, H.; Müller, K.-H.; Zürn, G. *Z. Anorg. Allg. Chem.* **1956**, *15*, 285.
(6) Schnering, H. G. v.; Menge, G. *Z. Anorg. Allg. Chem.* **1976**, *422*, 219.
(7) Gibinski, T.; Cisowaska, E.; Zdanowivz, W.; Henkie, Z.; Wojakowski, A. *Krist. Tech.* **1974**, *9*, 161.
(8) Maslout, A. E.; Zanne, M.; Jeannot, F.; Gleitzer, C. *J. Solid State Chem.* **1975**, *14*, 85.
(9) Gerardin, R.; Aubry, J.; Courtois, A.; Protas, J. *Acta Crystallogr., Sect. B: Struct. Crystallogr. Cryst. Chem.* **1977**, *B33*, 2091.
(10) Flörke, U.; Jeitschko, W. *J. Less-Common Met.* **1982**, *86*, 247.
(11) Olofsson, O. *Acta Chem. Scand.* **1965**, *19*, 229.
(12) Möller, M. H.; Jeitschko, W. *Z. Anorg. Allg. Chem.* **1982**, *491*, 225.
(13) Odile, J. P.; Soled, S.; Castro, C., A.; Wold, A. *Inorg. Chem.* **1978**, *17*, 283.
(14) (a) Ugai, Y. A.; Pshestanchik, V. R.; Anokhin, V. Z.; Gukov, O. Y. *Izv. Akad. Nauk. SSSR, Neorg. Mater.* **1974**, *10*, 405. (b) Juza, R.; Bär, K. *Z. Anorg. Allg. Chem.* **1956**, *283*, 230. (c) Goryunova, N. A.; Orlov, V. M.; Sokolova, V. I.; Shpenkov, G. P.; Tsvetkova, E. V. *Phys. Status Solidi* **1968**, *25*, 513. (d) Haraldsen, H. *Z. Anorg. Allg. Chem.* **1939**, *240*, 337.
(15) Zdanowicz, W.; Wojakowski, A. *Phys. Status Solidi* **1966**, *16*, K129.
(16) Jansen, M. *Angew. Chem., Int. Ed. Engl.* **1987**, *26*, 1098.
(17) Brown, A.; Rundqvist, S. *Acta Crystallogr.* **1965**, *19*, 684.
(18) Burdett, J. K.; McLarnan, T. *J. Chem. Phys.* **1981**, *75*, 5764.
(19) Jeitschko, W.; Flörke, M.; Scholz, M. *J. Solid State Chem.* **1984**, *52*, 320.
(20) Jeitschko, W.; Donohue, P. C. *Acta Crystallogr., Sect. B: Struct. Crystallogr. Cryst. Chem.* **1972**, *B28*, 1893.
(21) Alvarez, S.; Fontcuberta, J.; Whangbo, M.-H. *Inorg. Chem.* **1988**, *27*, 2702.
(22) Camus, A.; Marisch, N.; Nardin, G.; Randaccio, L. *Inorg. Chim. Acta* **1977**, *23*, 131.
(23) Mehrotra, P. K.; Hoffmann, R. *Inorg. Chem.* **1978**, *17*, 2187.
(24) Alemany, P.; Alvarez, S. To be submitted for publication.
(25) Cowley, A. H.; Jones, R. A.; Nunn, C. M.; Westmoreland, D. L. *Angew. Chem., Int. Ed. Engl.* **1989**, *28*, 1019.
(26) Jiang, Y.; Alvarez, S.; Hoffmann, R. *Inorg. Chem.* **1985**, *24*, 749.
(27) Komiya, S.; Albright, T. A.; Hoffmann, R.; Kochi, J. K. *J. Am. Chem. Soc.* **1977**, *99*, 8440.
(28) Dedieu, A.; Hoffmann, R. *J. Am. Chem. Soc.* **1978**, *100*, 2074.
(29) Mingos, D. M. P. *Proc. R. Soc. London, Ser. A* **1982**, *A308*, 75.
(30) Evans, D. G.; Mingos, D. M. P. *J. Organomet. Chem.* **1982**, *232*, 171.

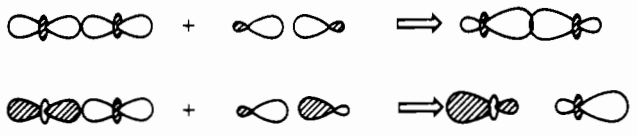

8

a small contribution from the s + p_z + d_{z^2} mixing. On the other hand, it would be interesting to see how the electronic band structure of such compounds correlates with the molecular orbital description of analogous isolated molecules. Therefore, we study first the local electronic structure and bonding of Cu_2X_6 models, and then look at the band structure of CuP_2.

Let us consider a hypothetical $[Cu_2Br_6]^{4-}$ ion in ethane-like (staggered, D_{3d} point group) and diborane-like (**7**, D_{2h} point group) structures and their interconversion via the geometrical rearrangement **9**. The molecular orbitals of the staggered compound

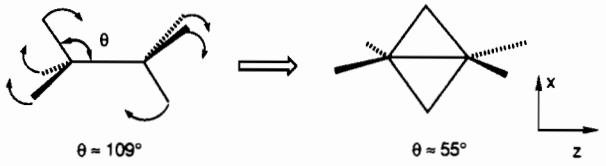

9

can be described from those of two pyramidal CuX_3 fragments, as schematically presented in Figure 1. The lowest occupied orbitals are those of σ_{Cu-X} character. Then come the "lone-pair" orbitals of the X atoms. At higher energy one finds the combinations of the Cu d orbitals; since they are all occupied for Cu(I), no contribution to Cu–Cu bonding results unless second-order effects are considered (see refs 23 and 26–30 for a detailed discussion on this subject). The lowest empty orbital of each CuX_3 fragment is a high-energy sp^3 hybrid, and the LUMO of $[Cu_2Br_6]^{4-}$ is therefore the bonding combination of such hybrids. With σ_{Cu-Cu} empty, the Cu–Cu overlap population is 0.089, comparable to that found for a d^{10}–d^{10} dinuclear compound (0.091) with a similar bond length (2.451 Å).[31]

Upon rearrangement of the ligands as in **9**, the LUMO is strongly destabilized, as the ligands moving toward bridging positions overlap with two instead of one copper atom (Figure 2, top). Since this orbital is metal-ligand antibonding, its bonding counterpart is stabilized. Therefore, for a Cu(I) compound, with the electron count shown in Figure 1, the diborane-like structure is expected to be more stable (Figure 2, bottom), in agreement with the local structure experimentally found for CuP_2 and AgP_2. Hence, the diborane-like coordination geometry of the d^{10} ions in CuP_2 is electronically favored. In fact, M_2X_2 diamonds of d^{10} metal ions are not uncommon, showing a wide range of M--M distances.[24] In d^{10} complexes with diborane-like structure, the delocalized bonding[24,32] is associated with the two occupied molecular orbitals a_g and b_{3u} shown in **10** and **11**.

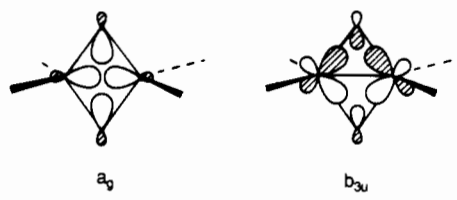

10 **11**

If one more electron per metal atom is added, as in Cu(0) or Zn(I), the LUMO becomes occupied. A *true* metal–metal bond is formed (Zn–Zn overlap population for $ZnBr_6^{4-}$ jumps to 0.40), and the ethane structure is expected to be more stable (Figure 2). This structure is found[33] in the isoelectronic anion $Sn_2P_6^{12-}$ present in $Ba_6Sn_2P_6$. It has also been reported for the monoclinic black form of ZnP_2, in which half of the Zn atoms are Zn(I)–Zn(I) pairs in Zn_2P_6 units with the staggered ethane structure.[34] Although Fleet and Mowles[35] have reexamined the structure of ZnP_2 and found it to be isostructural with $ZnAs_2$, the possibility of Zn(I)–Zn(I) bonds is theoretically sound.

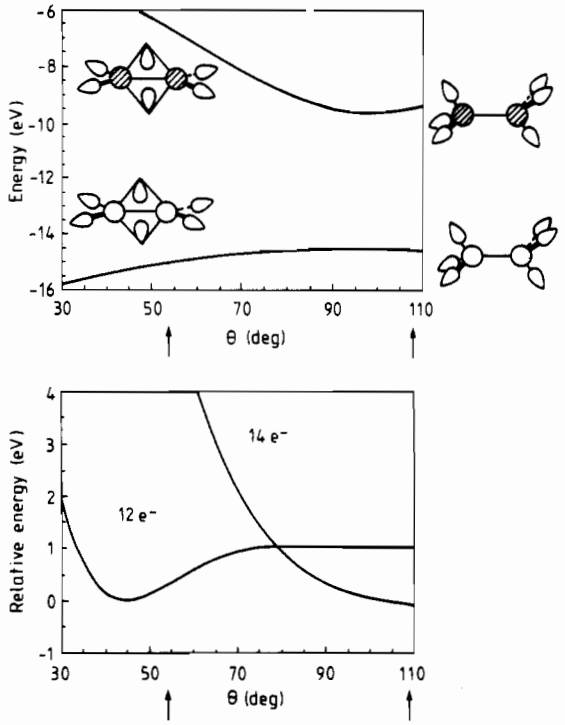

Figure 2. Top: Simplified Walsh diagram showing the energy variation of the HOMO and LUMO of $[Cu_2Br_6]^{4-}$ during the diborane (D_{2h}) → ethane (D_{3d}) distortion. Contributions from the p orbitals of Cu are omitted in the representation of the MO's for simplicity. Bottom: Energy variation for $[Cu_2Br_6]^{4-}$ (12 electrons) and the hypothetical 14-electron species isoelectronic with $[Zn_2Br_6]^{4-}$ for the same transformation. The arrow at 110° indicates the ethane-like structure, and the one at 54° the diborane-like structure.

Provided that the ligands are two-electron donors and the filled d orbitals are disregarded, the number of valence electrons in $[Cu_2X_6]^{4-}$ and $[Zn_2X_6]^{4-}$ (12 and 14, respectively) are the same as in B_2H_6 and C_2H_6. Thus, it is not surprising to find that the geometry preference is similar in both pairs of compounds. A detailed discussion of the orbital control of the diborane–ethane transformation can be found in the literature.[36,37] Comparison of these works with our discussion shows that the geometry preference is the same in both cases, but the orbital explanation is somewhat different. In A_2H_6 (A = C, B) the geometrical preference can be ascribed to the $1b_{2g}$ orbital, since it is A–H bonding and occupied in ethane but A–H nonbonding and empty in diborane (**12**). Namely, an additional bonding orbital is created

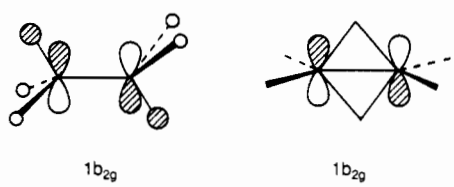

12

(31) Brown, I. D.; Dunitz, J. D. *Acta Crystallogr.* **1961**, *14*, 480.
(32) Summerville, R. H.; Hoffmann, R. *J. Am. Chem. Soc.* **1976**, *98*, 7240.
(33) Eisenmann, B.; Jordan, H.; Schäfer, H. *Z. Naturforsch. B: Anorg. Chem. Org. Chem.* **1983**, *38*, 404.
(34) Hegyi, I. J.; Laebner, E. E.; Poor, E. W.; White, J. G. *J. Phys. Chem. Solids* **1963**, *24*, 333.
(35) Fleet, M. E.; Mowles, T. A. *Acta Crystallogr.* **1984**, *C40*, 1778.
(36) Gimarc, B. M. *Molecular Structure and Bonding*; Academic Press: New York, 1979.
(37) Hoffmann, R.; Williams, J. E., Jr. *Helv. Chim. Acta* **1972**, *55*, 67.

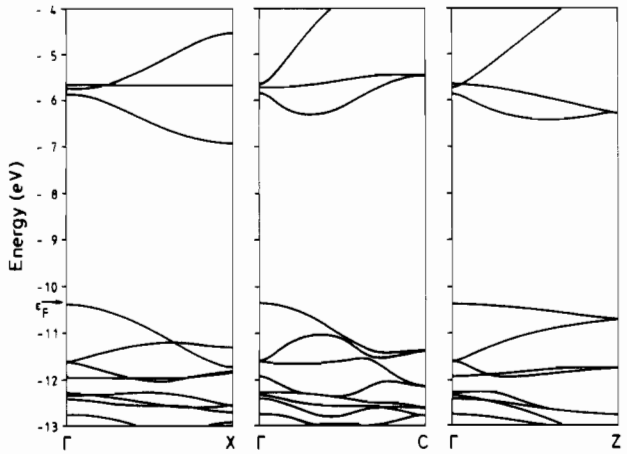

Figure 3. Dispersion relationships for CuP_2 along the most relevant symmetry lines of the Brillouin zone (**13**).

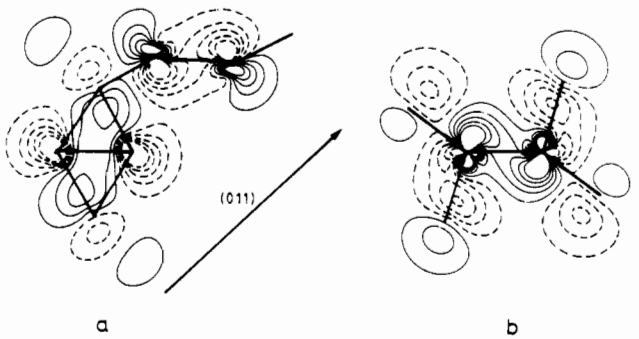

Figure 4. Contour diagrams for the highest occupied band at the Γ point: (a) projection showing the connection of the relevant fragment orbital of a Cu_2P_6 unit in the (011) direction; (b) projection showing the connectivity along the *a* (interlayer) direction.

in ethane to make room for the two extra electrons. In the M_2X_6 compounds, however, the $1b_{2g}$ orbital is mostly localized on the X atoms due to electronegativity reasons, thus remaining occupied for both structures. The geometrical preference is related to the conversion of localized M–X interactions into a stronger, delocalized M_2X_2 interaction (Figure 2, top).

Electronic Band Structure of CuP_2

Tight-binding electronic band structure calculations of the extended Hückel type were carried out on CuP_2 using the geometry of the experimental structure (see Appendix for computational details). Dispersion relations along several symmetry lines of the Brillouin zone **13** (BZ) are shown in Figure 3. All bands lying

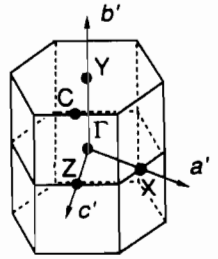

13

below −10 eV are filled, and the empty ones are separated by an indirect band gap of ~3.5 eV. The valence band has its highest energy at the Γ point and goes down in all directions of the BZ. This band is dispersive not only along ΓZ and ΓC, which correspond to the interactions within a layer in the real structure, but also along the ΓX line of the BZ, corresponding to the interlayer direction *a* in real space. The dispersive nature of this band would lead to a good conductivity of holes[38] created through any of three

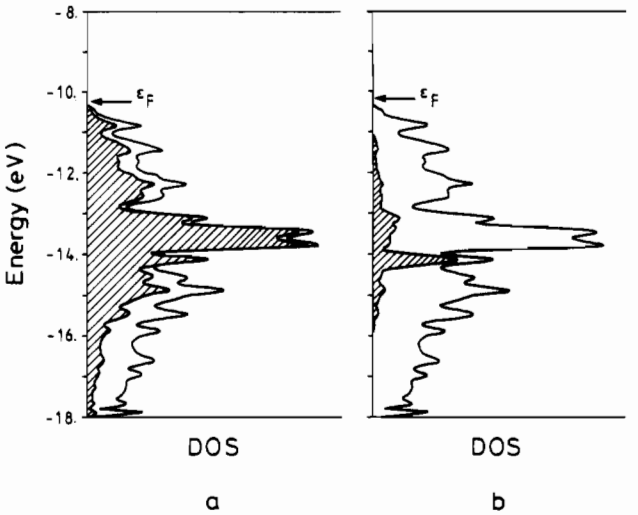

Figure 5. Calculated density of states for CuP_2. The shaded areas correspond to (a) the total contribution of the Cu atomic orbitals and (b) the contribution of the d_{z^2} orbitals of one of the two Cu_2 pairs in the unit cell.

mechanisms: thermal activation, radiative activation, or partial oxidation. While p-type semiconductivity[13] has been observed for CuP_2, photoconductivity or partial oxidation have not been reported so far.

To understand the dispersive nature of the highest occupied band, one must analyze its orbital composition. In Figure 3 the highest occupied crystal orbital occurs at the Γ point of the BZ. Within each layer (*bc* plane), the Cu_2P_6 units are connected as shown in **14**. One of the bridging P atoms of a Cu_2P_2 diamond

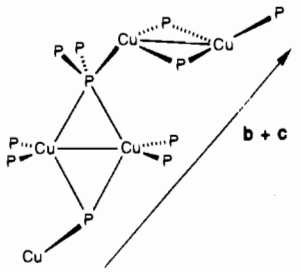

14

is also coordinated as a terminal ligand to a copper atom of the next diamond in the (011) direction, the planes of both diamonds being approximately perpendicular to each other. Hence, each P^- atom, linked to two phosphorus atoms, is used as a terminal ligand to one copper atom, formally contributing one electron pair to the bonding in the diborane-like Cu_2P_2 unit. The relevant fragment orbital of a Cu_2P_6 unit, formally a nonbonding orbital, is shown in Figure 4a as a contour diagram. The uppermost filled band is built up from the antibonding combination of such fragment orbitals (Figure 4a) from the two diamonds in the unit cell, as schematically shown in **15**. At the Γ point, the combi-

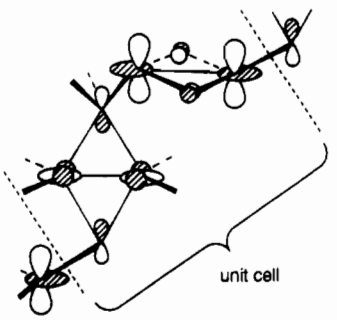

15

nation of nearest-neighbor orbitals **15** has Cu–P antibonding

(38) Cox, P. A. *The Electronic Structure and Chemistry of Solids*; Oxford University Press: Oxford, England, 1987; p 97.

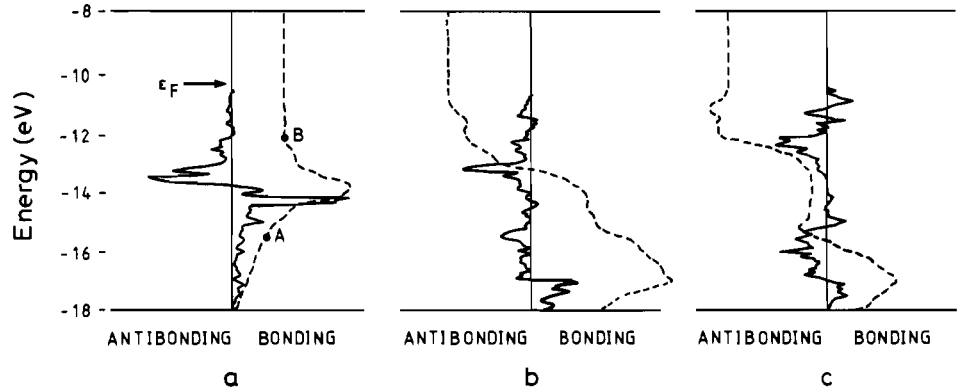

Figure 6. COOP curves for the interaction between Cu atoms (a), Cu s orbitals (b), and bridging phosphorus p_y orbitals (c). The integrated COOP's are represented by the dashed lines, the full scale corresponding to the values 0.22, 0.02, and 0.02 for curves a, b, and c, respectively. Points A anb B in (a) indicate the integrated Cu–Cu overlap population before and after filling the d_{z^2} band, respectively.

character, so that the band orbital at Γ is high in energy. As the phase is changed on going from Γ to C, the intercell antibonding character is gradually changed to bonding and the band levels become more stable. Similarly, the Cu_2P_2 diamonds are connected along the *a* direction (interlayer direction) as shown in **16** or, more

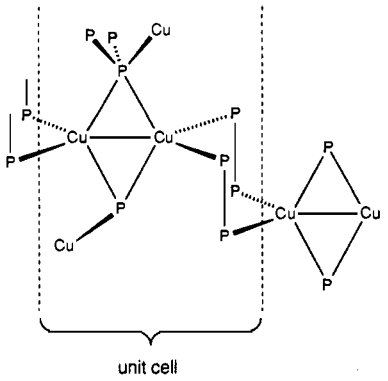

16

schematically, in **17**, where the phosphorus atoms of the diamond

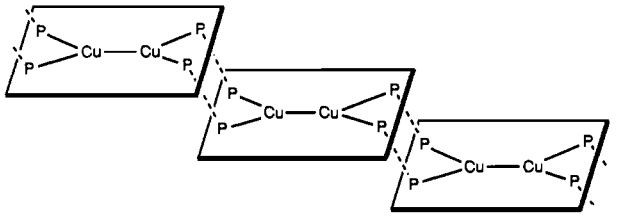

17

have been omitted for clarity. The fragment orbital (Figure 4b) is repeated in-phase along *a*, as in **18**, clearly bearing phospho-

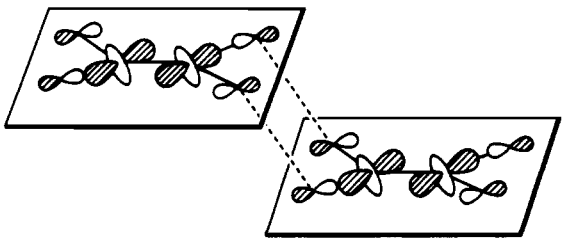

18

rus–phosphorus π-antibonding character. The dispersion of the valence band along the interlayer direction is due to through-bond coupling of the metal d orbitals (formally one of the nonbonding orbitals of the e set in a tetrahedral ligand field of phosphorus atoms). Important participation of the phosphorus atoms in the highest occupied levels has already been proposed, on the basis of X-ray emission spectra.[39-42]

The calculated density of states (DOS) is presented in Figure 5, together with the total contribution of the Cu atomic orbitals (shaded area in Figure 5a) and that of d_{z^2} of one of the Cu_2 pairs in the unit cell (shaded area in Figure 5b). In the DOS, a large gap (~3.5 eV) exists, in qualitative agreement with the semiconducting nature of CuP_2 and AgP_2. According to the projection of the Cu levels in the DOS plot (Figure 5a), the levels below the Fermi level (ϵ_F) are mostly centered in the copper atoms, although significant contributions from phosphorus atoms exist near ϵ_F, in agreement with both X-ray emission and photoelectron spectra.[39-42] Also the levels above ϵ_F (not shown in Figure 5) are mainly copper-centered.

The COOP curve (COOP stands for crystal orbital overlap population[43-45]) for the Cu–Cu bond (Figure 6a) shows both bonding and antibonding contributions below the Fermi level, in the region of the d orbitals, but the integrated Cu–Cu overlap population remains positive. Thus *there is* some Cu–Cu bonding, and the calculated overlap population (0.085) is quite similar to that found for unsupported dinuclear complexes with clearly established d^{10}–d^{10} interaction[23,26-30] (0.091 for the triazenido compound discussed above[31]). To examine if the same bonding scheme (**8**) applies to CuP_2, we repeated the band calculations excluding the copper d orbitals. The calculated Cu–Cu overlap population turns out to be roughly reduced to half (0.048), which indicates that both the delocalized diborane-like interaction and the $s + p_z + d_{z^2}$ mixing contribute to the Cu–Cu bonding. This result is consistent with the recent finding that in Cu_2X_2 diamonds the importance of the d^{10}–d^{10} bonding increases with decreasing Cu–Cu distances across the ring.[24] Since the coexistence of both types of bonding interaction in the solid state has not been studied previously, it is interesting to go through a more detailed analysis of the DOS and COOP curves.

Let us try first to identify the mixing of s, p_z, and d_{z^2} orbitals characteristic of unsupported bonding in dinuclear compounds of d^{10} ions. The contribution of the d_{z^2} orbitals to the band levels is seen in Figure 5 to be spread between −16 and −11 eV, with the major components at ca. −14 and −13 eV. These levels are built up from σ, Cu–Cu bonding (up to ~−13.8 eV), or σ* orbitals,

(39) Nefedov, V. I.; Salyn, Y. V.; Domashevskaya, E. P.; Ugai, Y. A.; Terekhov, V. A. *J. Electron Spectrosc. Rel. Phenom.* **1975**, *6*, 231.
(40) Domashevskaya, E. P.; Terekhov, V. A.; Marshakova, L. N.; Ugai, Y. A. *Izv. Akad. Nauk. SSSR, Ser. Fiz.* **1974**, *38*, 567.
(41) Domashevskaya, E. P.; Nefedov, V. I.; Salyn, Y. V.; Sergushin, N. P.; Terekhov, V. A.; Marshakova, L. N.; Ugai, Y. A. *Izv. Akad. Nauk. SSSR, Ser. Fiz.* **1976**, *40*, 389.
(42) Domashevskaya, E. P.; Terekhov, V. A.; Ugai, Y. A.; Nefedov, V. I.; Sergushin, N. P.; Dolenko, G. N. *Fiz. Tverd. Tela (Leningrad)* **1977**, *19*, 3610.
(43) Hughbanks, T.; Hoffmann, R. *J. Am. Chem. Soc.* **1983**, *105*, 3528.
(44) Wijeyesekera, S. D.; Hoffmann, R. *Organometallics* **1984**, *3*, 949.
(45) Hoffmann, R. *Solids and Surfaces: A Chemist's View of Bonding in Extended Structures*; VCH Publishers: New York, 1988.

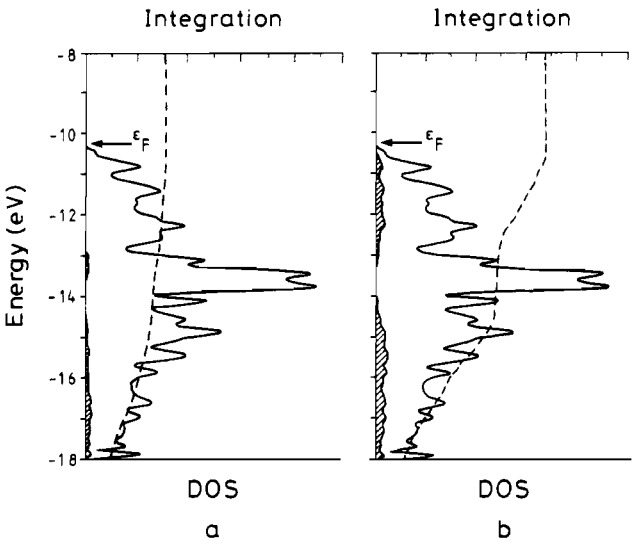

Figure 7. Calculated density of states for CuP_2. The shaded areas correspond (a) to the contribution of the s orbitals of Cu and (b) to the contribution of the p_y orbitals of the bridging phosphorus atoms. The integrated density of states for both projections is represented as a dashed line, the full scale corresponding to 100%.

Table I. Atomic Parameters for Extended Hückel Calculations[a]

atom	orbital	H_{ii}	ζ_{i1} (c_1)	ζ_{i2} (c_2)	ref
Cu	4s	−11.4	2.20		50
	4p	−6.06	2.20		
	3d	−14.0	5.95 (0.5933)	2.30 (0.5744)	
P	3s	−18.6	1.75		32
	3p	−14.0	1.30		
Br	4s	−22.07	2.588		51
	4p	−13.10	2.131		

[a] H_{ii}'s are the orbital ionization energies, ζ_{ij}'s the Slater exponents, and c_j's the coefficients in the double-ζ expansion of the d orbitals.

as seen in the COOP curve (Figure 6a). What is important to notice is that the Cu–Cu overlap population shows a net increase after filling both the σ and σ^* levels (cf. points A and B in Figure 6a). In other words, there is more Cu–Cu bonding character in the σ-band levels than antibonding character in the σ^* ones, a result which can be only explained by taking into account the s + p_z + d_{z^2} mixing typical of d^{10}–d^{10} bonding interactions.

The delocalized bonding orbitals of the M_2X_2 diamond (**10**, **11**) are found in the band levels below −16 eV. One finds DOS contributions from the phosphorus p_y and the copper s and p_z orbitals but little d contributions in this energy region (Figure 7). According to the corresponding COOP curves (Figure 6b,c), these levels are Cu--Cu and Cu-bridging P bonding, while the lowest ones (below −17 eV) are slightly P--P bonding and the upper ones (between −14 and −17 eV) are P--P antibonding, as expected for **10** and **11**, respectively. In fact, the wave function at the center of the Brillouin zone (Γ point) with an energy of −18.09 eV is formed by the combinations of a_g orbitals (**10**), and those at −15.72 and −15.49 eV at the same point are built up from b_{3u} orbitals (**11**).

In summary, both molecular orbital and band structure calculations indicate that the bonding in the M_2X_2 diamonds of CuP_2 and AgP_2 presents the features of delocalized bonding typical of diborane as well as the d^{10}–d^{10} interactions characteristic of unsupported dinuclear Au(I) and Cu(I) complexes. The electrical properties of such compounds are predicted to be isotropic and are related to M–M nonbonding d orbitals coupled through P_2 bridges.

Acknowledgment. Financial support for the research at Barcelona was given by the CICYT through Grant PB89-0268. We are grateful to F. Vilardell for the drawings. P.A. thanks the Ministerio de Educación y Ciencia for a fellowship of the Plan Nacional de Nuevos Materiales. Work at North Carolina State University was supported by the Office of Basic Energy Sciences, Division of Material Sciences, U.S. Department of Energy, under Grant DE-FG05-86ER45259.

Appendix: Computational Details

The qualitative theoretical discussions in this paper are based on molecular orbital[46] and tight-binding band calculations[47,48] of the extended Hückel type with modified Wolfsberg–Helmholz formula,[49] using the atomic parameters shown in Table I. MO calculations were carried out on the model compound $[Cu_2Br_6]^{4-}$, using the following bond distances: Cu–Br = 2.30 Å; Cu–Cu = 2.48 Å; Br–Cu–Br angles = 109°. Average properties of CuP_2 were calculated using a set of 48 k points chosen according to the geometrical method of Ramírez and Böhm.[52]

Registry No. CuP_2, 12019-11-3.

(46) Hoffmann, R. *J. Chem. Phys.* **1963**, *39*, 1397. Hoffmann, R.; Lipscomb, W. N. *J. Chem. Phys.* **1962**, *36*, 2179, 2872, 3489.
(47) Whangbo, M.-H.; Hoffmann, R. *J. Am. Chem. Soc.* **1978**, *100*, 6093.
(48) Whangbo, M.-H.; Hoffmann, R.; Woodward, R. B. *Proc. R. Soc. London, Ser. A* **1979**, *366*, 23.
(49) Ammeter, J. H.; Bürgi, H.-B.; Thibeault, J. C.; Hoffmann, R. *J. Am. Chem. Soc.* **1978**, *100*, 3686.
(50) Hay, P. J.; Thibeault, J. C.; Hoffmann, R. *J. Am. Chem. Soc.* **1975**, *97*, 4884.
(51) Alvarez, S.; Mota, F.; Novoa, J. *J. Am. Chem. Soc.* **1987**, *109*, 6586.
(52) Ramírez, R.; Böhm, M. C. *Int. J. Quantum Chem.* **1988**, *34*, 571. Ramírez, R.; Böhm, M. C. *Int. J. Quantum Chem.* **1986**, *30*, 391.